OPTIMIZATION OF PHYSICAL PROPERTY AND WORKING CONDITION PARAMETERS IN MULTI-SIZE SINTER VERTICAL TANK BASED ON EXERGY ANALYSIS

Si-Zong ZHANG [1], Lin-Jing HUANG [1,*], Zhi WEN [1], Xun-Liang LIU [1]

[1] School of Energy and Environmental Engineering, University of Science and Technology Beijing, Beijing, 100083, China

[*] Corresponding author; E-mail: hlj1075051083@163.com

Aiming at the characteristics of multi-size particles in the waste heat recovery sinter vertical tank, a steady-state gas-solid heat transfer model of multi-size vertical tank was established. Based on exergy analysis, the influences of physical properties and working conditions on the gas-solid heat transfer and the waste heat recovery capacity of the vertical tank were studied. Finally, the optimum parameter combination was obtained by the orthogonal test method. Results showed that the mono-size sinter was no longer suitable for analyzing the gas-solid heat transfer process of the vertical tank in the actual production. The total exergy of the multi-size sinter vertical tank increased first and then decreased with the increase of aspect ratio in the range of 0.39-1.75, and reaches the peak value when height-diameter ratio is 0.7. The total exergy increased with the increase of temperature difference between gas-solid inlet temperature. The total exergy increased first and then decreased with the increase of gas-material ratio in the range of 610-1170 $m^3 \cdot t^{-1}$, and reached the maximum value at the gas-material ratio of 850 $m^3 \cdot t^{-1}$. The exergy decreased with the increase of porosity in the range of 0.548-0.603. The most suitable vertical tank parameters were as follows: height-diameter ratio 0.44, sinter inlet temperature 800 ℃, gas inlet temperature 25 ℃, gas-material ratio 770 $m^3 \cdot t^{-1}$ and porosity 0.601.

Key words*: sinter vertical tank, waste heat recovery, orthogonal test method, exergy analysis, numerical simulation, parameter optimization*

1.Introduction

The energy consumption of iron and steel industry is large, among which the energy consumption of sintering process accounts for about 15 % of the total energy consumption. Most of the sintering flue gas is not recovered and utilized, but directly discharged into the atmospheric environment [1]. In view of the disadvantages of the traditional sinter waste heat recovery process, such as high air leakage rate, partial recovery of waste heat, and low outlet air energy level, scholars put forward the waste heat recovery technology of sinter vertical tank based on the dry coke quenching process [2, 3, and 4]. The technology can increase the waste heat recovery rate from 40 % to 80 % and can make full use of the waste heat energy of sinter. This is of great significance to the development goals of energy conservation, emission reduction, and carbon neutrality.

At present, the waste heat recovery technology of sinter vertical tank has gradually stepped into the engineering demonstration stage, but the numerical study of sinter vertical tank is mainly aimed at single-size sinter. In actual production, the sinter is characterized by wide particle size distribution, so the sinter vertical tank is essentially a packed bed with multi-size particle mixing [5]. Zhang [6] et al. studied the gas resistance characteristics in the multi-size sinter vertical tank and obtained the correlation formula for predicting gas resistance. The results showed that the correlation formula of single-size resistance was not applicable to multi-size sinter. Gas-solid heat transfer and gas resistance are two key factors in the packed bed study. However, there are few reports on the gas-solid heat transfer of multi-size sinter vertical tank. In the field of single-size sinter vertical tank, most scholars take exergy value as evaluation index to analyze the main factors and laws that affect gas-solid heat transfer characteristics and waste heat recovery ability [7]. Dong [8] et al. first introduced the exergy transfer coefficient of the convection heat exchanger and packed bed into the waste heat recovery process of vertical tank and derived the formula of exergy transfer coefficient in bed layer. Zhao [9] et al. compared the heat recovery effect of circular cooling and vertical tank cooling modes through exergy analysis, and found that the vertical tank cooling mode could greatly improve the sinter sensible heat recovery, with exergy efficiency reaching 75.39 %, which is nearly 20 % higher than that of circular cooling mode. Feng and Zhang [10, 11, and 12] et al. introduced the exergy efficiency analysis model of vertical tank, and analyzed the influences of sinter inlet temperature, equivalent particle size, and material ratio on exergy output in vertical tank waste heat recovery process. Liu [13] et al. further simulated the influence of sinter porosity on exergy output in the vertical tank waste heat recovery process through COMSOL Multiphysics.

Based on porous media theory and gas-solid heat transfer theory, the exergy analysis method is introduced into the study of gas-solid heat transfer in multi-size sinter vertical tank, and a two-dimensional steady-state gas-solid heat transfer model is established. Tridiagonal matrix algorithm method (TDMA) is used to solve the temperature field iteratively, and then the residual heat recovery capacity of vertical tank is evaluated by exergy value. On this basis, this paper analyzes the effects of physical properties and working parameters on gas-solid heat transfer characteristics and waste heat recovery capacity of multi-size sinter vertical tank, and carries out the optimization analysis of parameters in the vertical tank by using orthogonal test method, and obtains the appropriate parameter settings of the vertical tank. This study aims to lay a foundation for the further engineering implementation of sinter vertical tank waste heat recovery technology in actual production.

2.Gas-solid heat transfer model of vertical tank

2.1.Physical model and hypothesis

Referring to the physical structure characteristics of dry quenching furnace, a physical model of vertical tank body structure is constructed, as shown in Fig. 1. The sinter particles enter the pre-storage section from the top, and are cooled by heat exchange with the retrograde cooling air in the cooling section, and then discharged from the bottom of the tank. The cooling air is pumped into the bottom of the vertical tank by the fan, and heat exchange occurs with the hot sinter in the cooling section. The high-temperature flue gas obtained enters the waste heat boiler for heat exchange with the condensed water, and the condensed water becomes superheated steam, which then enters the steam turbine for power generation.

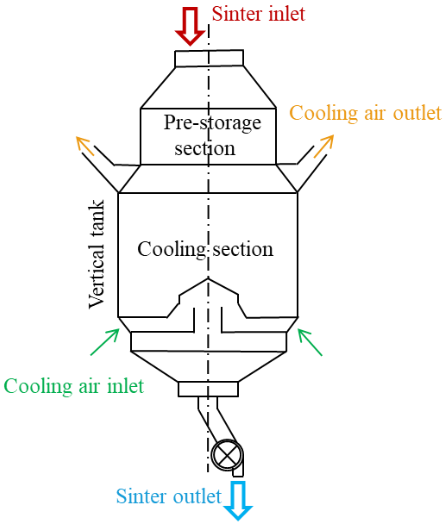

Fig. 1 Physical model of the sinter vertical tank

The forced convective heat transfer process of cooling air in the pore of cooling bed is complicated. So it is an effective way to simplify it reasonably. Several assumptions are as follows [4]:

1) Only the axial and radial temperature changes are considered, and the two-dimensional axisymmetric model is used instead of the three-dimensional model.
2) Because the sinter particle size is much smaller than the structure size of the vertical tank, the bed is regarded as a porous medium moving at a constant speed.
3) The sinter downward velocity is small and the relative velocity of gas and solid is constant, so the gas-solid heat transfer process of air passing through the pore of the bed is similar to the steady heat transfer process of fluid passing through the porous medium [14].
4) Due to the temperature difference between adjacent sinters or sinter and gas is small, the influence of radiation heat transfer is ignored.

2.2.Mathematical model

Based on the gas-solid heat transfer theory, the thermophysical properties of air and sinter are far apart and there is always a temperature difference between them. Therefore, air and solid temperature are regarded as two independent variables and a local thermal non-equilibrium double energy equation is adopted [14]. According to the law of energy conservation, the control equation of gas-solid heat transfer in the vertical tank are as follows:

Gas phase region:

$$\frac{\partial(\rho_{\mathrm{g}}v_{\mathrm{g}}c_{\mathrm{pg}}T_{\mathrm{g}})}{\partial z}=\varepsilon\left[\frac{1}{r}\frac{\partial}{\partial r}(\lambda_{\mathrm{g}}r\frac{\partial T_{\mathrm{g}}}{\partial r})+\frac{\partial}{\partial z}(\lambda_{\mathrm{g}}\frac{\partial T_{\mathrm{g}}}{\partial z})\right]+S_{\mathrm{pv}}\alpha(T_{\mathrm{s}}-T_{\mathrm{g}}) \tag{1}$$

Solid phase region:

$$\frac{\partial(\rho_{\mathrm{s}}v_{\mathrm{s}}c_{\mathrm{ps}}T_{\mathrm{s}})}{\partial z}=\left(1-\varepsilon\right)\left[\frac{1}{r}\frac{\partial}{\partial r}(\lambda_{\mathrm{s}}r\frac{\partial T_{\mathrm{s}}}{\partial r})+\frac{\partial}{\partial z}(\lambda_{\mathrm{s}}\frac{\partial T_{\mathrm{s}}}{\partial z})\right]+S_{\mathrm{pv}}\alpha(T_{\mathrm{g}}-T_{\mathrm{s}}) \tag{2}$$

where g and s represent gas and solid; ρ is the true density, kg·m^{-3}; v_{g} and v_{s} are apparent velocities, m·s^{-1}; T is the temperature, K; c_{p} is the specific heat capacity, J·(kg·K)$^{-1}$; λ is the thermal conductivity, W·(m·K)$^{-1}$; S_{pv} is the specific surface area; α is the convective heat transfer coefficient, W·(m^2·K)$^{-1}$; The porosity ε is calculated using the density measured in the experiment [15]:

$$\varepsilon=1-\frac{\rho_{\mathrm{b}}}{\rho_{\mathrm{a}}} \tag{3}$$

where ρ_{b} and ρ_{a} respectively represent the apparent density measured by drainage method and the bulk density measured by direct weighing method, kg·m^{-3}.

Convective heat transfer coefficient α can be calculated by Eq. (4):

$$\alpha=\frac{\mathrm{Nu_e}\lambda_{\mathrm{g}}}{d_{\mathrm{p}}} \tag{4}$$

where d_{p} is equivalent sinter particle size, m; $\mathrm{Nu_e}$ is Nusselt number, which is calculated by using the gas-solid heat transfer correlation formula of multi-size sinter fitted by experiment:

$$\mathrm{Nu_e}=0.006961\left(\frac{1-\varepsilon}{\varepsilon}\right)^{0.9185}\mathrm{Re}^{1.1703}\mathrm{Pr}^{1/3} \tag{5}$$

This paper uses C# language to compile the program on Microsoft Visual Studio platform. Half of the cross-section along the central axis of the cooling section is cut off as the calculation domain, and the region is divided into $m \times n$ parts along the height z and radius r axes. The grid division form is shown in Fig. 2. The double energy equations of gas and solid are discretized into alternating implicit difference scheme and the algebraic equations are arranged into tridiagonal matrix form. The TDMA method is used to solve the energy equation iteratively and the steady-state temperature field in the vertical tank can be obtained by minimization of residuals. A detailed solution algorithm can be found in reference [16], which can simulate the gas-solid heat transfer process of multi-size sinter vertical tank.

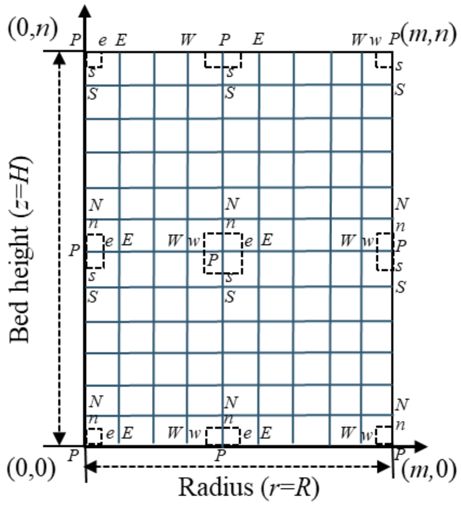

Fig. 2 Schematic diagram of the TDMA method grid partitioning

2.3.Boundary conditions

1) The radial central axis (r=0) is set as the adiabatic boundary condition:

$$-\lambda_{\rm g}\nabla T_{\rm g}\big|_{r=0}=0,\quad -\lambda_{\rm s}\nabla T_{\rm s}\big|_{r=0}=0 \tag{6}$$

2) The radial outer surface (r=R) conducts natural convection and radiation heat transfer with the outer air, so it is set as the third boundary condition:

$$\lambda_{\rm g}\frac{\partial T_{\rm g}}{\partial r}\bigg|_{r=R}=h_{\rm a}(T_{\rm a}-T_{\rm g}),\quad \lambda_{\rm s}\frac{\partial T_{\rm s}}{\partial r}\bigg|_{r=R}=h_{\rm a}(T_{\rm a}-T_{\rm s}) \tag{7}$$

where R is the radius of the outer boundary, m; $T_{\rm a}$ is the ambient temperature, K; $h_{\rm a}$ is the natural convective heat transfer coefficient between the wall and the environment [17], W·(m^2·K)$^{-1}$:

$$h_{\rm a}=\frac{{\rm Nu}_{\rm a}\lambda_{\rm g}}{d_{\rm p}} \tag{8}$$

where ${\rm Nu}_{\rm a}$ can be calculated according to different application scopes:

$$\begin{cases} \mathrm{Nu_a} = 0.68 + \dfrac{0.67(\mathrm{GrPr})^{1/4}}{\left[1+(0.492/\mathrm{Pr})^{9/16}\right]^{4/9}} & \mathrm{GrPr} < 10^9 \\ \mathrm{Nu_a}^{1/2} = 0.825 + \dfrac{0.387(\mathrm{GrPr})^{1/6}}{\left[1+(0.492/\mathrm{Pr})^{9/16}\right]^{8/27}} & \mathrm{GrPr} > 10^9 \end{cases} \tag{9}$$

where Gr is the Grashof number, approximately the ratio of viscous force and buoyancy force, which can be calculated by

$$\mathrm{Gr} = \frac{g\beta(T_\mathrm{w} - T_\mathrm{e})L^2}{v^2} \tag{10}$$

where β is the gas expansion coefficient, and for ideal gas $\beta \approx 1/\left(273.15 + T_\mathrm{e}\right)$, K^{-1}; T_w is the wall temperature, ℃; v is the gas kinematic viscosity coefficient, $m^2 \cdot s^{-1}$; g is the gravity acceleration, $m \cdot s^{-2}$.

3) Axial surface ($z=H$) :

The sinter moves downward at the constant sinter inlet temperature $T_\mathrm{s,in}$, and the air is set as adiabatic condition:

$$T_\mathrm{s}\big|_{z=H} = T_\mathrm{s,in}, \quad -\lambda_\mathrm{g}\nabla T_\mathrm{g}\big|_{z=H} = 0 \tag{11}$$

where H is the height of vertical tank bed, m.

4) Axial downward surface ($z=0$) :

The air is blown at constant inlet air temperature $T_\mathrm{g,in}$, and the sinter is set as adiabatic condition:

$$T_\mathrm{g}\big|_{z=0} = T_\mathrm{g,in}, \quad -\lambda_\mathrm{s}\nabla T_\mathrm{s}\big|_{z=0} = 0 \tag{12}$$

2.4.Exergy analysis model

When evaluating the waste heat recovery capacity of sinter vertical tank, the traditional first law of thermodynamics only considers the change of total energy. Exergy, as a parameter to comprehensively evaluate the value of energy, defines the “value” of energy in terms of “quality” and “quantity” based on the first and second laws of thermodynamics, better revealing the essence of internal loss [17]. As only gas flow and gas-solid heat transfer are involved in sinter vertical tank, the physical exergy is mainly considered in calculation. Exergy analysis in the multi-size sinter vertical tank simulation region is shown in Fig. 3.

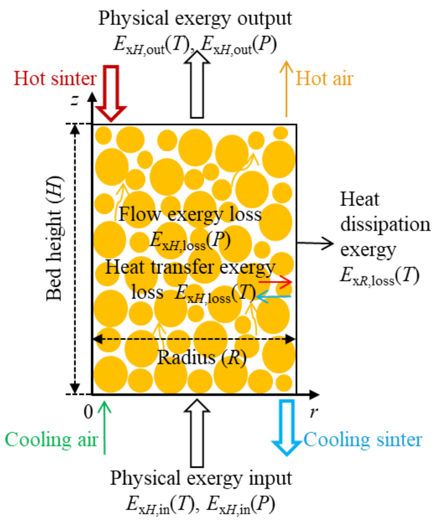

Fig. 3 Exergy analysis diagram of the vertical tank cooling section

The temperature exergy is used to represent the "quantity" and "quality" of exergy heat carrier, that is, the maximum available energy for subsequent turbogenerator generation [18, 19, and 20]:

$$E_{xH,\mathrm{out}}(T) = q_{\mathrm{g}} \int_{T_{\mathrm{g,in}}}^{T_{\mathrm{g,out}}} c_{\mathrm{pg}} (1 - \frac{T_{\mathrm{a}}}{T}) dT \tag{13}$$

where q_{g} is gas mass flow rate, kg·s^{-1}[21].

The pressure exergy of heat carrier is used to represent the pressure loss of vertical tank:

$$E_{xH,\mathrm{out}}(P) = q_g R_g T_0 \ln \frac{P_{\mathrm{out}}}{P_0} \tag{14}$$

where P_{out} is the outlet gas pressure, generally the atmospheric pressure, and P_0 is the inlet gas pressure, Pa. According to the correlation formula of airflow resistance in the multi-size sinter filled bed fitted with experimental results, the bed airflow pressure drop ΔP is as follows [22]:

$$\Delta P = P_0 - P_{\mathrm{out}} = \frac{(2843/\mathrm{Re} + 5.29)}{d_{\mathrm{p}}\varepsilon^3 / \left[(1-\varepsilon)(\rho_{\mathrm{g}} v_{\mathrm{g}}^2 H)\right]} \tag{15}$$

where Re is the Reynolds number.

As the overall reference index, the comprehensive recovery benefit $E_{xH,\mathrm{out}}$ is given as

$$E_{xH,\mathrm{out}} = E_{xH,\mathrm{out}}(T) + E_{xH,\mathrm{out}}(P) = q_g [\int_{T_{\mathrm{g,in}}}^{T_{\mathrm{g,out}}} c_{\mathrm{pg}} (1 - \frac{T_{\mathrm{a}}}{T}) dT + R_g T_0 \ln \frac{P_{\mathrm{out}}}{P_0}] \tag{16}$$

3.Parameter Setting

In this paper, a batch of 5 – 60 mm sinter particles from No.2 sintering machine of Handan Iron and Steel Group Company are used as the multi-size mixing materials for the experiment. It is screened into 11 groups of single-size sinter with different particle size distribution and mixed according to different mass fractions. Six groups of multi-size sinter mixtures are obtained and related physical parameters are measured, as shown in Tab. 1 and Tab. 2. On this basis, the real distribution of particles in vertical tank is simulated by random distribution in the program.

Based on the equivalent ball volume method, the particle size of single-size sinter is characterized by equivalent particle size [21]:

$$d_{\mathrm{p,si}} = \left(\frac{6m_{\mathrm{p,si}}}{\pi \rho_{\mathrm{s,si}}} \right)^{1/3} \tag{17}$$

where si represents the *i*-th single-size sinter; m_{p} is the average sinter mass measured in the experiment, kg.

In actual production, the multi-size sinter is randomly distributed and has certain particle size distribution, so the average particle size with harmonized quality is used to represent:

$$d_{\mathrm{p,m}} = \sum_{i=1}^{n} w_{i,\mathrm{si}} \Big/ \sum_{i=1}^{n} \frac{w_{i,\mathrm{si}}}{d_{\mathrm{p,si}}}$$

(18)

where m represents the multi-size sinter; $w_{i,\mathrm{si}}$ is the mass fraction, %.

The apparent density of multi-size sinter $\rho_{\mathrm{a,m}}$ can be obtained by weighting the apparent density of each single-size sinter:

$$\rho_{\mathrm{a,m}} = \sum_{i=1}^{n} w_{i,\mathrm{si}} \rho_{\mathrm{a,si}} \tag{19}$$

Table 1 Physical parameters of the single-size sinter

Particle size/mm	$w_{i,\mathrm{si}}$ /%	$d_{\mathrm{p,si}}$ /mm	$\rho_{\mathrm{a,si}}$ /(kg·m^{-3})	$\rho_{\mathrm{b,si}}$ /(kg·m^{-3})
(5 – 10]	24.6	5.6	3847.6	1643.9
(10 – 15]	19.6	10.9	3726.4	1513.4
(15 – 20]	13.6	14.5	3656.3	1448.7
(20 – 25]	10.6	19.2	3614.6	1419.5
(25 – 30]	8.0	23.3	3561.8	1382.8
(30 – 35]	7.1	26.8	3547.1	1359.2
(35 – 40]	4.9	30.8	3536.3	1342.5
(40 – 45]	3.7	35	3526.8	1327.6
(45 – 50]	2.7	38.5	3523.4	1306.1

(50 – 55]	2.5	43.3	3523.1	1297.2
(55 – 60]	2.7	47.4	3522.7	1282.1

Table 2 Related physical parameters of the multi-size sinter

Group number	$d_{p,m}$ /mm	$\rho_{a,m}$ /(kg·m^{-3})	$\rho_{b,m}$ /(kg·m^{-3})	ε
Group 1	11.2	3676.1	1663.5	0.548
Group 2	15.2	3622.0	1581.0	0.564
Group 3	19.2	3589.7	1513	0.579
Group 4	23.2	3569.2	1455.6	0.592
Group 5	27.2	3553.9	1421.4	0.601
Group 6	31.2	3543.4	1408.2	0.603

4.Model verification

In order to verify the accuracy of the model, the data of single-size sinter test conditions measured by sinter vertical tank test device in literature [22] are compared with the simulation results in this paper, as shown in Tab. 3. It can be found that the relative errors (%) of the gas and solid outlet temperature are all within 10 %, which meets the requirements of engineering accuracy. The established model can accurately simulate the gas-solid heat transfer process in the sinter vertical tank.

Table 3 Comparison of the numerical simulation results and experimental measurement results

Test conditions			Test results		Numerical simulation results			
$T_{s,in}$	q_s /(kg·s^{-1})	q_{vg} /(m^3·h^{-1})	$T_{s,out}$	$T_{g,out}$	$T_{s,out}$	Error	$T_{g,out}$	Error
1006	0.5	1545	381	751	349	8.3	745	0.8
1021	0.5	1641	377	723	345	8.5	748	3.5
1147	0.6	1723	417	904	437	4.8	870	3.8
1110	0.6	1859	397	799	390	1.8	828	3.6
1003	0.6	1646	398	829	411	3.3	772	6.9
1167	0.7	1925	423	922	457	8.0	905	1.8

5.Results and discussions

Based on the actual production condition of the sinter vertical tank [23], the basic working parameters are set: sinter and gas inlet temperatures are 700 ℃ and 20 ℃, sinter output is 550 t·h^{-1}, gas-material ratio is 691 m^3·t^{-1}, height and diameter of vertical sinter tank are 7 m and 9 m.

5.1. Temperature field distribution

Based on the setting of basic working conditions, Fig. 4 compares the gas-solid temperature field distribution of the multi-size and single-size sinter vertical tanks with porosity of 0.579. It reveals that the temperature distribution of multi-size sinter fluctuates significantly compared with that of single-size sinter, which is more consistent with the actual operating conditions. The gas outlet temperature of single-size sinter is 66 ℃, while that of multi-size sinter is 60 ℃. The heat exchange effect of multi-size sinter vertical tank is better that of single-size sinter vertical tank, because the large difference in size characteristics of multi-size sinters increases the residence time of gas between the pores of sinter, thus enhancing the heat exchange effect. Therefore, the theoretical system of single-size sinter is no longer suitable for analyzing the gas-solid heat transfer process of multi-size sinter vertical tank.

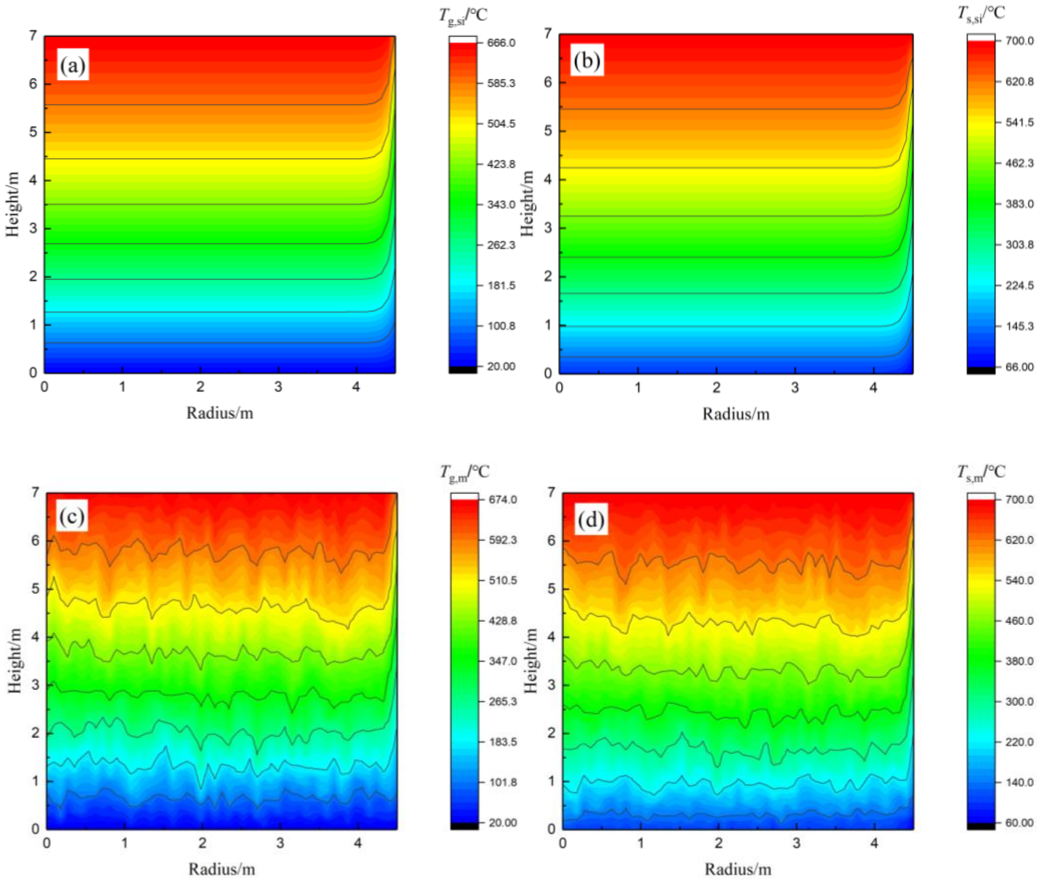

Fig. 4 Temperature field distribution of the multi-size and single-size sinter vertical tank: (a) $T_{g,si}$; (b) $T_{s,si}$; (c) $T_{g,m}$; (d) $T_{s,m}$

The influence of factors such as height-diameter ratio, sinter and gas inlet temperature, gas-material ratio, and porosity on waste heat recovery ability of multi-size sinter vertical tank is analyzed by using control variable method in the following part, and the optimum parameter combination is obtained by using orthogonal test method. The purpose is to provide reference for engineering practice.

5.2. Influence of height-diameter ratio on exergy value

On the basis of the basic working condition, the porosity of the vertical tank is set as 0.579, and the height-diameter ratio is adjusted in the range of 0.39-1.17. Fig. 5 shows the change of pressure exergy, temperature exergy, and total exergy with the height-diameter ratio of the vertical tank. Fig. 5(a) shows the pressure exergy increases with the increase of height-diameter ratio. As the resistance of the gas passing through the material layer increases, and the pressure loss also increases gradually. Fig. 5(b) shows the temperature exergy increases with the increase of the height-diam eter ratio, but the increase will gradually slow down after the height-diameter ratio is 0.7. Therefore, the overall exergy value in Fig. 5(c) increases first and then decreases with the increase of the height-diameter ratio, and reaches the peak value when the height-diameter ratio is 0.7. This is because the contact heat transfer time between the sinter and the air is prolonged, and the heat transfer is more sufficient and gradually tends to saturation. However, the continuous accumulation of pressure loss will reduce the availability of the system, thus weakening the waste heat recovery ability of the vertical tank. The structure of "squat shape" is more beneficial to improve the waste heat recovery effect of vertical tank than that of "thin and tall shape".

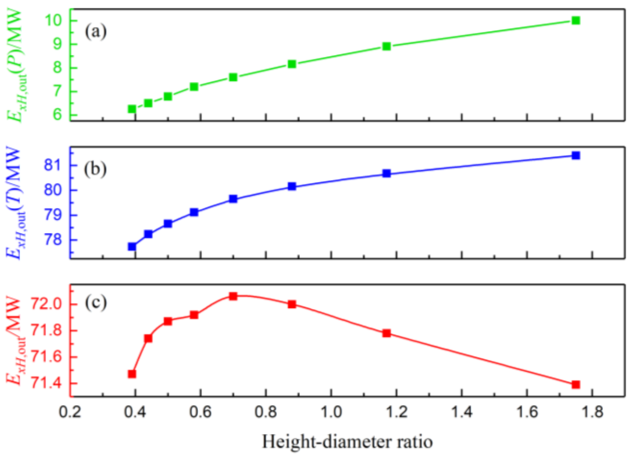

Fig. 5 Effect of the height-diameter ratio on waste heat recovery of vertical tank: (a) $E_{xH,\text{out}}(P)$; (b) $E_{xH,\text{out}}(T)$; (c) $E_{xH,\text{out}}$

5.3. Influence of gas and solid inlet temperature on exergy value

Based the basic working condition, the height-diameter ratio is set at 0.7, and the gas and solid inlet temperature is adjusted within the range of 5-40 ℃ and 500-850 ℃, respectively. Fig. 6 and Fig. 7 show the change of the pressure exergy, temperature exergy, and total exergy with inlet gas and sinter temperature, respectively. Fig. 6(a) and Fig. 7(a) show that the pressure exergy increases with the increase of gas and solid inlet temperature. However, Fig. 6(b, c) and Fig. 7(b, c) show that the temperature exergy and total exergy decreases with the increase of inlet gas temperature, and increases with the increase of inlet sinter temperature. This is because the temperature difference between the overall gas-solid heat exchange of the vertical tank will increase, thus enhancing the heat exchange effect. Although increasing the gas and solid inlet temperature can reduce the bed pressure loss, the overall residual heat recovery capacity of the vertical tank is determined by the temperature exergy caused by the temperature difference. The greater the temperature difference is, the better the residual heat recovery effect is.

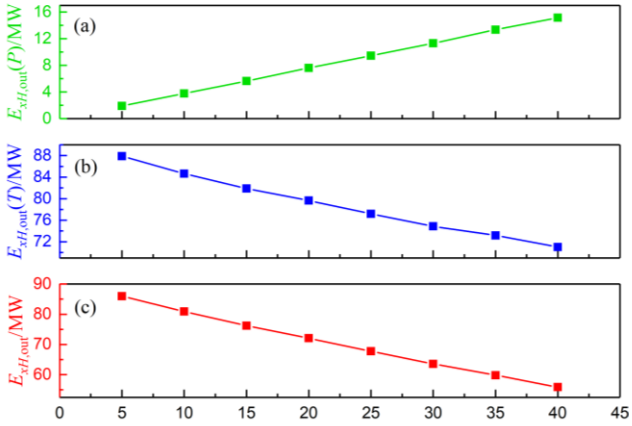

Fig. 6 Effect of the inlet gas temperature on waste heat recovery of vertical tank

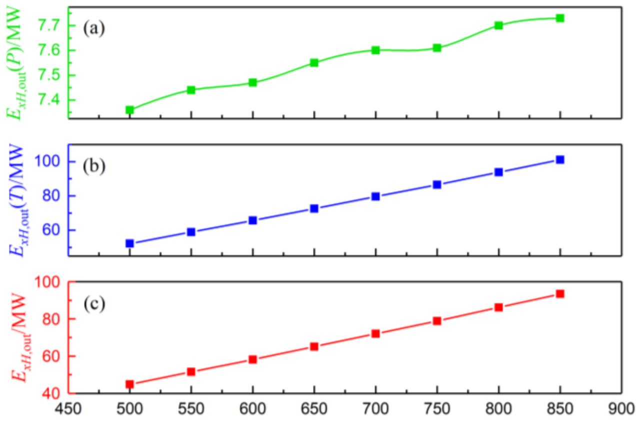

Fig. 7 Effect of the inlet sinter temperature on waste heat recovery of vertical tank

5.4. Influence of gas-material ratio on exergy value

Based on the basic working conditions, the gas-material ratio is adjusted in the range of 610-1170 $m^3 \cdot t^{-1}$. Fig. 8 shows the change of the pressure exergy, temperature exergy, and total exergy with the gas-material ratio of the vertical tank. It shows that the pressure exergy increases linearly with the increase of gas-material ratio. The temperature exergy increases first with the increase of gas-material ratio, and there is a slight downward trend after the gas-material ratio of 850 $m^3 \cdot t^{-1}$. Therefore, the overall exergy increases first and then decreases with the increase of gas-material ratio, and reaches the maximum value when the gas-material ratio is 850 $m^3 \cdot t^{-1}$. This is because the heat exchange between gas and sinter becomes more sufficient with the increase of gas flow rate, and the heat carried by the gas outlet keeps increasing.

However, the vertical heat recovery ability is limited when the gas flow rate increases further, and the pressure loss caused by gas flow plays a dominant role, thus reducing the overall exergy value of the gas outlet.

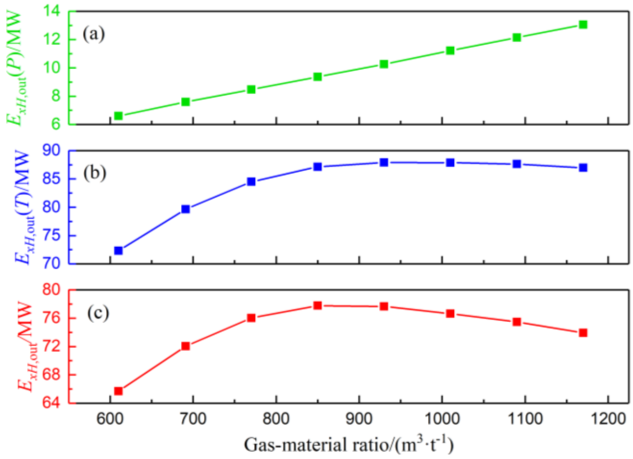

Fig. 8 Effect of the gas-material ratio on waste heat recovery of vertical tank

5.5. Influence of porosity on exergy value

Based on the basic working condition, the porosity is adjusted in the range of 0.548-0.603 $m^3 \cdot t^{-1}$. Fig. 9 shows the change of the pressure exergy, temperature exergy, and total exergy with porosity. It shows that the pressure exergy, temperature exergy and total exergy value all decreases with the increase of porosity, and when the porosity is greater than 0.601, the decrease of the exergy value increases. This is because under the same sinter output, the diameter of sinter particles increases with the increase of porosity, and the surface area of particles decreases relatively, thus reducing the contact area between sinter and air and weakening the convective heat transfer effect between sinter particles and air. The internal thermal resistance of sinter will also increase because of the increase of thermal conductivity thickness, thus reducing the heat transfer rate from sinter to air. To sum up, the increase of porosity within a certain range will reduce the waste heat recovery effect of sinter vertical tank.

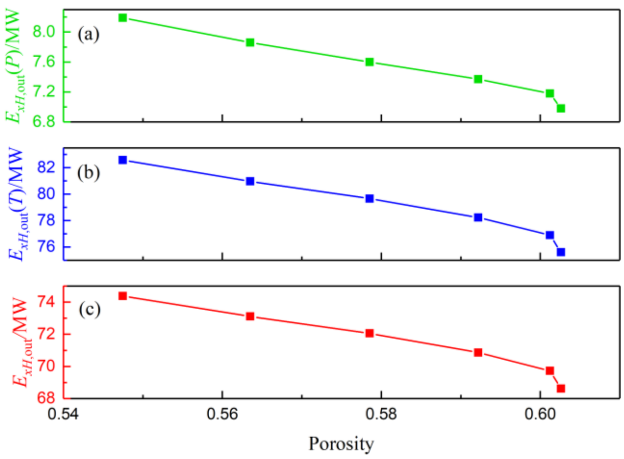

Fig. 9 Effect of porosity on waste heat recovery of vertical tank

5.6. Parameter optimization

The orthogonal test method is an efficient experimental design method for arranging multi-factor experiments and seeking optimal combination of levels. In this paper, the orthogonal test method is used to systematically analyze the influences of the five main parameters, such as height-diameter ratio, gas-solid inlet temperature, gas-material ratio, and porosity, on the total exergy value of sinter vertical tank, so as to obtain the most suitable parameter combination. Therefore, the orthogonal test table U12(6^5), that is, orthogonal test of 5 factors, 6 levels and 12 working conditions, is selected for the optimization analysis, as shown in Tab. 4.

Table 4 Orthogonal test table $U_{12}(6^5)$

Working condition	Parameter					$E_{xH,out}$ /MW
	Height-diameter ratio	Sinter inlet temperature /℃	Gas inlet temperature /℃	Gas-material ratio /($m^3 \cdot t^{-1}$)	porosity	
	Level					
Test 1	1.17	750	20	1010	0.603	30.21
Test 2	0.58	750	35	850	0.564	103.45
Test 3	0.88	550	25	1090	0.564	29.26
Test 4	0.50	600	20	691	0.548	118.12
Test 5	0.70	800	15	930	0.548	100.63
Test 6	0.58	550	15	850	0.603	82.75
Test 7	0.50	700	30	1090	0.592	124.80
Test 8	0.70	600	35	930	0.601	46.55
Test 9	0.88	700	10	691	0.592	50.95
Test 10	0.44	650	10	1010	0.579	203.95
Test 11	1.17	650	30	770	0.579	21.43
Test 12	0.44	800	25	770	0.601	214.76

Tab. 5 shows the orthogonal test results of total exergy obtained by the theoretical range analysis. I_i, II_i, III_i, IV_i, V_i, and VI_i represent the mean test results of parameter *i* at levels 1, 2, 3, 4, 5, and 6, respectively. R_i is the range of parameter *i*, that is, the difference between the best level and the worst level of parameter *i*, and represents the influence degree of parameter *i* on the test results. The larger R_i value is, the greater the influence degree of parameter *i* on the test results is, and vice versa [24]. Tab. 5 shows the influence of different parameters on the test results: $R_1>R_3>R_2>R_5>R_4$. Therefore, the most suitable parameter combination is as follows: height-diameter ratio 0.44, sinter inlet temperature 800 ℃, gas inlet temperature 25 ℃, gas-material ratio 770 $m^3 \cdot t^{-1}$, and porosity 0.601.

Table 5 Orthogonal test results

	Parameter				
	Height-diameter ratio	Sinter inlet temperature/℃	Gas inlet temperature/℃	Gas-material ratio/($m^3 \cdot t^{-1}$)	porosity
I_i : Mean level 1 test results	209.4	56.0	254.9	84.5	109.4
II_i : Mean level 2 test results	121.5	82.3	91.7	118.1	66.4
III_i : Mean level 3 test results	93.1	112.7	74.2	93.1	112.7
IV_i : Mean level 4 test results	73.6	87.9	122.0	73.6	87.9
V_i : Mean level 5 test results	40.1	66.8	73.2	117.1	130.7
VI_i : Mean level 6 test results	25.8	157.7	75.0	77.0	56.5
R_i : range	183.5	101.7	181.7	44.5	74.2

6.Conclusions

Based on the porous media theory and gas-solid heat transfer theory, a two-dimensional steady-state gas-solid heat transfer model is established. The relative errors between simulation and experimental values of sinter and gas outlet temperature are all within 10 %, which meet the requirements of engineering accuracy. The main conclusions obtained through exergy analysis are as follows:

1) The temperature distribution of multi-size sinter fluctuates significantly compared with that of single-size sinter, which is more consistent with the actual operating conditions. The theoretical system of single-size sinter is no longer suitable for analyzing the gas-solid heat transfer process of multi-size sinter vertical tank.
2) The total exergy increases first and then decreases with the increase of the height-diameter ratio from 0.39 to 1.75, and reaches the maximum value when the height-diameter ratio is 0.7. The “squat shape” structure is more conducive to waste heat resources recovery of vertical tank. The total exergy increased with the increase of temperature difference between gas-solid inlet temperature. In the range of 610-1170 $m^3 \cdot t^{-1}$, the gas-material ratio increases first and then decreases with the increase of the gas-material ratio, and reaches the maximum value when the gas-material ratio is 850 $m^3 \cdot t^{-1}$. The exergy decreases with the increase of porosity in the range of 0.548-0.603.
3) The influence of parameter combination optimization on waste heat recovery of vertical tank is considered by the orthogonal test. It shows that parameters have different influences on the total exergy: height-diameter ratio > gas inlet temperature > solid inlet temperature > porosity > gas-material ratio. The most suitable vertical tank parameters should be set as: height-diameter ratio 0.44, sinter inlet temperature 800 ℃, gas inlet temperature 25 ℃, gas-material ratio 770 $m^3 \cdot t^{-1}$ and porosity 0.601.

Acknowledgements

This work is supported by Fundamental Research Funds for the Central Universities (FRF-TP-22-077A1).

References

[1] Li L., Experimental Study on Exergy Transfer Coefficient of Layer in Vertical Tank for Recovering Sinter Waste Heat (Master thesis in Chinese), Northeastern University, Shenyang, China, 2013

[2] Feng J.S., Study on Gas-solid Heat Transfer Model in Vertical Tank for Recycling Sinter Waste Heat (Master thesis in Chinese), Northeastern University, Shenyang, China, 2014

[3] Liu W.Y., *et al*., Numerical Simulation of Cooling Process in Vertically-arranged Sinter Coolers (in Chinese), *Conservation and Utilization of Mineral Resources*, (2018), No.4, pp: 63-68

[4] Liu Y., *et al*., Prediction, Parametric Analysis and Bi-objective Optimization of Waste Heat Utilization in Sinter Cooling Bed Using Evolutionary Algorithm, *Energy*, (2015), No.90, pp: 24-35

[5] Tian F.Y., *et al*., Experimental Study on Pressure Drop of Packed Beds with Binary Sintered Ore Particle Mixtures (in Chinese), *Journals of Zhejiang University (Engineering Science)*, 50(2016), No.11, pp: 2077-2085

[6] Zhang S.Z., *et al*., Gas Resistance Characteristics in Vertical Tank with Irregular Sinter for Waste Heat Recovery (in Chinese), *Journal of Central South University (Science and Technology)*, 52(2021), No.6, pp: 1063-1072

[7] Zhang X.H., *et al*., Optimization and Simulation of Sinter Cooling Process, *CIESC Journal*, 62(2011), No.11, pp: 3081-3087

[8] Dong H., *et al*., Experimental Study on Exergy Transfer Coefficient Affected by Cooling Air Volume in Vertical Tank of Waste Heat Recovery (in Chinese), *Journal of Northeastern University (Natural Science)*, 35(2014), No.5, pp: 708-711

[9] Zhao M.R., *et al*., Utilization of Remaining Exergy of Sintering Cooling System Based on Exergy Analysis Method (in Chinese), *Iron and Steel*, 53(2018), No.7, pp: 89-94

[10] Feng J.S., *et al*., Numerical Simulation and Optimization of Gas-solid Heat Transfer Process in Sinter Vertical Tank (in Chinese), *Journal of Northeastern University (Natural Science)*, 37(2016), No.11, pp: 1559-1563

[11] Zhang S., *et al*., Optimization of Operating Parameters of Sinter Waste Heat Vertical Tank Based on Exergy Efficiency (in Chinese), *Journal of Central South University (Science and Technology)*, 52(2021), No.4, pp: 1287-1296

[12] Feng J.S., *et al*. Numerical Analysis of Gas-solid Heat Transfer Process in Vertical Tank for Sinter Waste Heat Recovery (in Chinese), *Journal of Central South University (Science and Technology)*, 48(2017), No.11, pp: 3100-3107

[13] Liu W.Y., *et al*. Numerical Simulation of Cooling Process in Vertically-arranged Sinter Coolers (in Chinese), *Conservation and Utilization of Mineral Resources*, (2018), No.4, pp: 63-68

[14] Feng J.S., Gas Solid Heat Transfer Process and Application Research in Vertical Tank for Sinter Waste Heat Recovery (Master thesis in Chinese), Northeastern University, Shenyang, China, 2017

[15] Zhang S.Z., Study on Flow and Heat Transfer Characteristics in the Sinter Vertical Cooling Process (Master thesis in Chinese), University of Science and Technology Beijing, Beijing, China, 2021

[16] Moawwad El-Mikkawy, and Faiz Atlan, A Novel Algorithm for Inverting a General K-tridiagonal Matrix, *Applied Mathematics Letters*, (2014), No.32, pp: 41-47

[17] Koekemoer A., and Luckos A., Effect of Material Type and Particle Size Distribution on Pressure Drop in Packed Beds of Large Particles: Extending the Ergun Equation, *Fuel*, (2015), No.158, pp: 232

[18] Zhang S., *et al*, Parameter Optimization of Gas-solid Heat Transfer Process in Sinter Packed Bed Based on Further Exergy Analysis, *Chemical Engineering Research and Design*, (2019), No.146, pp: 499−508

[19] Feng H.J., *et al*. Constructal Optimization of a Sinter Cooling Process Based on Exergy Output Maximization, *Applied Thermal Engineering*, (2016), No.96, pp: 161-166

[20] Liu Y., *et al*. Energy and Exergy Analysis for Waste Heat Cascade Utilization in Sinter Cooling Bed, *Energy*, (2014), No.67, pp: 370-380

[21] Yan L., *et al*. Experimental Investigation of Fluid Flow and Heat Transfer in a Randomly Packed Bed of Sinter Particles, *International Journal of Heat and Mass Transfer*, (2016), No.99, pp: 589-598

[22] Zhang S.Z., *et al*., Experimental Study on the Permeability and Resistance Characteristics in the Packed Bed with the Multi-size Irregular Particle Applied in the Sinter Vertical Waste Heat Recovery Technology, *Powder Technology*, (2021), No.384, pp: 304-312

[23] Tao B.B., *et al*. Porous Media's Drying Model of Non-equilibrium Themodynamics (in Chinese), *Journal of Hebei University of Technology*, 34 (2005), No.1, pp: 109-112

[24] Zhang J.Y., *et al*. Optimal Orthogonal Simulation Research of Sinter Cooling (in Chinese), *Iron and Steel*, 46(2011), No.7, pp: 86-89

Submitted:	17.09.2022
Revised:	16.12.2022
Accepted:	28.12.2022